

Bifurcations in the rotational spectra of odd nuclei

I. M. Pavlichenkov

I. V. Kurchatov Institute of Atomic Energy

(Submitted 9 January 1989)

Zh. Eksp. Teor. Fiz. **96**, 404–417 (August 1989)

A critical phenomenon, of which bifurcation is the classical analog, has been found in the rotational bands of highly-deformed odd nuclei. Analysis of the classical and quantum-mechanical pictures of the phenomenon shows that it is accompanied by a change in correlation between the total and single-nucleon angular momentum vectors. The qualitative changes found in the energy spectrum and electromagnetic $M1$ transition probabilities can be used to demonstrate the quantum-mechanical bifurcation in high-spin states of odd nuclei. Experimental data that indicate the existence of bifurcation in the bands of odd-neutron isotopes of ytterbium are presented.

1. INTRODUCTION

As the excitation energy of a nucleus increases, the dynamics of its internal motion becomes increasingly complicated because of the increasing importance of nonlinear effects. The interaction of quasiparticles with one another and with other degrees of freedom complicates the nuclear energy spectrum to the extent that one can speak of dynamic chaos. However, even before this, at much lower excitation energies, dynamic nonlinear effects should lead to bifurcations that produce a qualitative change in the energy spectrum of one of the nuclear excitation branches. Certain detailed properties of single-particle motion, deformation, and other structure factors manifest themselves in the neighborhood of the bifurcation point.

Bifurcations in many-particle systems have not been extensively investigated. They are usually identified with second-order phase transitions which, in contrast to thermodynamic phase transitions, are referred to as ground-state phase transitions because, in the classical limit, the second derivative of the ground-state energy of the system with respect to some parameter exhibits a discontinuity at the critical value of this parameter. This picture has been used to analyze critical points of the energy shell that is obtained by averaging the quantum-mechanical Hamiltonian over the coherent state with the corresponding symmetry. This method was originally developed for the Lipkin model with $SU(2)$ symmetry¹ and has been used to investigate phase transitions in phenomenological algebraic models such as those of interacting bosons [$SU(6)$ symmetry]² and fermions with $SU(8)$ dynamic symmetry.³

Studies of quantum-mechanical bifurcations have been mostly confined to simple model systems^{4,5} in which bifurcations are due to the appearance of a well with two degenerate minima as the potential parameters are varied. In a previous paper, written in collaboration with Zhilinskii,⁶ we investigated the critical phenomena that arise in the rotational spectra of quantum-mechanical systems under the influence of centrifugal forces. The essence of the phenomenon is that, for a sufficiently high angular momentum, systems that do not have axial symmetry exhibit a change in the dynamics of precessional motion, which is seen as a regrouping of a part of the rotational multiplet (RM—a set of rotational states with given angular momentum I) when the critical point I_c is reached. In the classical limit, critical phenomena are associated with bifurcations in the Hamiltonian system

with a particular type of local symmetry. The transition parameter is then the angular momentum—a constant of motion of the system. Of the five types of critical phenomena that can occur in purely rotational spectra, two are “local.” They are characterized by the appearance of RM clusters, i.e., almost degenerate levels corresponding to the delocalization of precession around equivalent axes. Local critical phenomena are universal near I_c : they occur in a limited region of phase space and are described by a closed Hamiltonian with a small number of parameters that depend on the internal structure of the system.

Critical phenomena were predicted⁷ and discovered⁸ when the rotational spectra of certain spherical molecules (CH_4 , SiH_4 , and SnH_4) were analyzed. There is considerable interest in bifurcations in the upper part of the RM of water molecules and other symmetric triatomic molecules of the hydrates of group IV and group VI elements for angular momenta $I_c \sim 30$.⁹ As these molecules rotate around a stable axis with the minimum moment of inertia, the latter increases with increasing I because of the centrifugal force. When its magnitude becomes comparable with the intermediate moment of inertia, the initial axis of rotation loses its stability. Two equivalent (because of the symmetry of the molecule) axes become stable and lie symmetrically on either side of the initial axis of rotation. There is no doubt that this phenomenon should also occur in nuclear rotational spectra because some nuclei become nonaxial for $I \sim 40$. However, the phenomenon is difficult to detect because the levels tend to bunch in the upper part of the multiplet, i.e., above the yrast region in which the density of levels with given spin is high.

Nonlinear effects in rotational spectra are due not only to centrifugal forces but also to Coriolis forces. The latter arise from the coupling between single-particle and rotational degrees of freedom. In nuclear physics, the Coriolis force manifests itself in the rotational spectra of odd nuclei, and is proportional to the single-particle nucleon angular momentum j . Consequently, the strongest coupling to rotation is experienced by nucleons occupying subshell levels with maximum j . These levels differ in parity from other states in the shell being filled. It follows that j is a good quantum number for them because the admixture of states with other values of j corresponds to transitions to a neighboring shell. The Coriolis force orients the vector \mathbf{j} along the total angular momentum \mathbf{I} of the nucleus. This gives rise to the so-

called decoupled bands that have now been discovered in many odd nuclei across the periodic table. The most extensively investigated are the decoupled bands of rare-earth nuclei in which the odd neutron or proton occupies the $i_{13/2}$ or $h_{11/2}$ subshells.

We shall show below that, for a particular occupancy of a subshell with anomalous parity, a transition to a decoupled band as I increases is accompanied by a quantum-mechanical bifurcation that can be observed as levels of different symmetry (signature) approach one another in a band, or by examining the change in the dependence of the M 1 probability on I near the critical point. A phenomenological theory of quantum-mechanical bifurcations has been developed and can be used to analyze the rotational spectra of odd nuclei near the critical point. The dependence of the energies and electromagnetic transition probabilities on signature has been used^{10,11} to extract information on the nonaxial properties of the nucleus in states with high angular momentum. The closeness of these states to the bifurcation point can substantially affect the results of the analysis.

2. EFFECTIVE HAMILTONIAN

Among the states of an odd axial nucleus, we consider a rotational band for which the odd nucleon occupies levels in an anomalous-parity subshell with given j . The total spin of the nucleus consists of the angular momentum of the core (\mathbf{R}) and that of the odd nucleon, i.e., $\mathbf{I} = \mathbf{R} + \mathbf{j}$. Consequently, for given j and each value of the nuclear spin, there are several levels forming the RM. Instead of the true nuclear Hamiltonian, we shall consider the effective Hamiltonian in the space of the RM states. In its most general form, it can be written in the intrinsic coordinate frame (ICF) as follows:

$$H = g_0(\mathbf{R}^2, \mathbf{j}^2) + \frac{1}{2} \sum_{k=1}^{\infty} [g_k(\mathbf{R}^2, \mathbf{j}^2); j_3^{2k}]_{+,} \quad (1)$$

where g_k are arbitrary functions, the first term is the rotational energy of the core, and the remaining terms represent the axisymmetric field in which the motion of the nucleon takes place and which depends on rotation.

Relative to the laboratory coordinate frame (LCF) the orientation of the axis of symmetry \mathbf{n} of the core that is parallel to the symmetry axis of the mean field is defined by the polar angles θ and ϕ . The orientation of axes 1, 2, and 3 of the ICF is chosen so that axis 3 lies along the vector \mathbf{n} . The ICF then coincides with the spheroidal coordinate system. The projections of the total angular momentum operator \mathbf{I} onto the ICF axes must therefore obey unusual commutation relations both with one another and with the projections of the operator \mathbf{j} (details may be found in Ref. 12, which discusses the nonadiabatic theory of diatomic molecules):

$$\begin{aligned} [I_1, I_2] &= -i(I_1 \operatorname{ctg} \theta + j_3), & [I_1, I_3] &= [I_2, I_3] = 0, \\ [j_1, I_1] &= -ij_2 \operatorname{ctg} \theta, & [j_2, I_1] &= ij_1 \operatorname{ctg} \theta, & [j_3, I_1] &= 0, \\ [j_k, I_2] &= 0, \quad k=1, 2, 3; & [j_1, I_3] &= -ij_2, & [j_2, I_3] &= ij_1, & [j_3, I_3] &= 0. \end{aligned} \quad (2)$$

The expression for the square of the angular momentum operator of the core,

$$\mathbf{R}^2 = \mathbf{I}^2 + \mathbf{j}^2 - 2j_3^2 - j_+ I_- - j_- I_+, \quad (3)$$

where $I_{\pm} = I_1 \pm iI_2$, $j_{\pm} = j_1 \pm ij_2$, can be obtained from the commutation rules (2). The conserved quantities for the Hamiltonian (1) are \mathbf{I}^2 , \mathbf{j}^2 , and the projection of \mathbf{I} onto the z axis of the LCF with quantum number M . This means that the eigenfunctions of the Hamiltonian H can be written in the form

$$\Psi_{IMn} = \sum_K a_{IKn} D_{MK}^I(\varphi, \theta, 0) |jK\rangle, \quad (4)$$

where D_{MK}^I is the Wigner function, $|jK\rangle$ is an eigenfunction of the operators \mathbf{j}^2 and j_3 , and the sum over the component K of the total angular momentum along axis 3 of the ICF runs from $-I$ to I for $I < j$ and from $-j$ to j for $I > j$. From now on, we shall be interested only in multiplets with $I > j$. The invariance of the function given by (4) under the transformation $\mathcal{R} = \exp[-i\pi(I_2 - j_2)]$ leads to the following expression for the expansion coefficients¹³

$$a_K = (-1)^{I-j} a_{-K}. \quad (5)$$

The function can therefore be written in the form

$$\begin{aligned} \Psi_{IMn} &= \sum_{K=1/2}^j a_{IKn} \{D_{MK}^I(\varphi, \theta, 0) |jK\rangle \\ &+ (-1)^{I-j} D_{M,-K}^I(\varphi, \theta, 0) |j-K\rangle\}. \end{aligned} \quad (6)$$

It follows that multiplet levels with different parity of $I - j$ have different symmetry properties under the rotation of the entire nucleus by 180° about ICF axis 2. In reactions involving heavy ions, in which the latter are used to excite the rotational states, only the lowest level of each multiplet is populated. The set of levels observed in a rotational band of an odd nucleus is usually split into two sequences, namely, those with even $I - j$ (favored band) and those with odd values of this difference (unfavored band). A conserved quantum number, i.e., the signature $\sigma = (-1)^{I-j}$ can be introduced for these two sequences.

3. CLASSICAL BIFURCATION

In the classical approximation, the energy of a level in a multiplet is determined by the mutual orientation of vectors \mathbf{R} and \mathbf{j} . In the lower part of the RM, the angle ϑ between these vectors is acute, whereas for the upper levels it is obtuse. For given I and j , the energy of the core-plus-nucleon system has the following form according to (1):

$$\begin{aligned} E(\vartheta, \phi) &= \sum_{k=0}^{\infty} (j \sin \vartheta \cos \phi)^{2k} \\ &\times g_k([(I^2 - j^2 \sin^2 \vartheta)^{1/2} - j \cos \vartheta]^2, j^2), \end{aligned} \quad (7)$$

where the orientation of the vector \mathbf{j} relative to the ICF is defined by angles ϑ and ϕ .

Stationary points of the energy surface (7) can be found from the equation

$$\begin{aligned} \{[(I^2 - j^2 \sin^2 \vartheta)^{1/2} - j \cos \vartheta]^2 A(\vartheta) + \\ + j \cos \vartheta (I^2 - j^2 \sin^2 \vartheta)^{1/2} C(\vartheta)\} \sin \vartheta \cos \phi = 0, \end{aligned} \quad (8)$$

where

$$\begin{aligned}
A(\vartheta) &= \sum_{h=0}^{\infty} (j \sin \vartheta \cos \phi)^{2h} \\
&\times g_k'([(I^2 - j^2 \sin^2 \vartheta)^{1/2} - j \cos \vartheta]^2, j^2), \\
C(\vartheta) &= \sum_{h=0}^{\infty} k (j \sin \vartheta \cos \phi)^{2(h-1)} \\
&\times g_k'([(I^2 - j^2 \sin^2 \vartheta)^{1/2} - j \cos \vartheta]^2, j^2), \quad (9)
\end{aligned}$$

and g_k' is the derivative of g_k with respect to \mathbf{R}^2 . The stationary point $\vartheta = 0$ corresponds to an aligned configuration of the angular momentum vectors:

$$I_1 = I, \quad I_2 = I_3 = 0, \quad j_1 = j, \quad j_2 = j_3 = 0, \quad \mathbf{R}^2 = R_-^2 = (I - j)^2, \quad (10)$$

where the energy

$$E_0(I) = g_0(R_-^2, j^2), \quad (11)$$

corresponds to the lowest RM level. The highest level corresponds to the anti-aligned configuration ($\vartheta = \pi$) that differs from (10) by the sign of the component j_1 .

To investigate the energy surface near an aligned configuration, let us expand the function $E(\vartheta, \phi)$ into a series, assuming that the angle ϑ is small, and write this expression in terms of the Cartesian coordinates $\xi = \vartheta \cos \phi$, $\eta = \vartheta \sin \phi$ near ICF axis 1:

$$E(\xi, \eta) = E_0(I) + a_{20}\xi^2 + a_{02}\eta^2 + a_{40}\xi^4, \quad (12)$$

where $a_{02} \sim g_0'(R_-^2, j^2) > 0$ and the coefficient $a_{20} \sim R_-^2 g_0'(R_-^2, j^2) + I j g_1(R_-^2, j^2)$ can vanish at the critical value of the total angular momentum, given by

$$I_c = j[1 - p + (p^2 - 2p)^{1/2}], \quad p = g_1/2g_0' \quad (13)$$

(we are assuming that g_0' and g_1 are smooth functions of the variable R_-). When this occurs, we have $a_{20} = a(I - I_c)$, near I_c , where $a > 0$. Consequently, for $I < I_c$, the minimum (10) of the surface (7) becomes a saddle point, and there are two additional degenerate minima lying on the 13 plane ($\phi_0 = 0, \pi$), symmetric with respect to axis 1. They correspond to the stationary states

$$\begin{aligned}
I_{10} &= (I^2 - j^2 \sin^2 \vartheta_0)^{1/2}, \quad I_{20} = 0, \quad I_{30} = \pm j \sin \vartheta_0, \\
j_{10} &= j \cos \vartheta_0, \quad j_{20} = 0, \quad j_{30} = I_{30}, \\
\mathbf{R}^2 &= R_0^2 = (I_{10} - j_{10})^2 \quad (14)
\end{aligned}$$

with energy

$$\tilde{E}_0(I) = \sum_{h=0}^{\infty} g_h(R_0^2, j^2) j_{30}^{2h}. \quad (15)$$

The angle $\vartheta_0 \neq 0$ is determined from (8). It is readily shown that $\tilde{E}_0''(I_c) - E_0''(I_c) \neq 0$.

The function given by (12) is the canonical form of the critical phenomenon for the local symmetry groups C_s , C_2 , or C_{2v} .⁶ However, in contrast to the bifurcation examined in Ref. 6, which is connected with a change in the precession

axis of a soft nonaxial spinning top, the phenomenon investigated here consists essentially of the change in the mutual orientation (i.e., the correlation), of the vectors \mathbf{I} , \mathbf{j} , and \mathbf{R} . This interpretation of the phenomenon becomes more obvious when we investigate the precessional motion of these vectors near the stationary points (10) and (14).

Let us now consider the classical equations of motion $\dot{X}_i = \{H, X_i\}$ for the components X_i of vectors \mathbf{I} and \mathbf{j} along the ICF axes, where H is the classical Hamiltonian (1) in which $\mathbf{R}^2 = (I_1 - j_1)^2 + (I_2 - j_2)^2$, and $\{\dots\}$ are Poisson brackets. Using Poisson brackets for the components of the angular momenta, which are the analog of the commutation rules (2), we can show that the complete set of equations of motion is

$$\begin{aligned}
\dot{I}_1 &= 2\{-(I_1 - j_1)j_2 \operatorname{ctg} \theta + (I_2 - j_2)[(I_1 - j_1) \operatorname{ctg} \theta + j_3]\} \\
&\times \sum_{h=0}^{\infty} g_k'(R^2, j^2) j_s^{2h}, \\
\dot{I}_2 &= 2(I_1 - j_1)(I_1 \operatorname{ctg} \theta + j_3) \sum_{h=0}^{\infty} g_k'(R^2, j^2) j_s^{2h}, \\
\dot{I}_3 &= \dot{j}_3 = 2(j_1 I_2 - I_1 j_2) \sum_{h=0}^{\infty} g_k'(R^2, j^2) j_s^{2h}, \\
\dot{j}_1 &= -2[(I_1 - j_1)j_2 \operatorname{ctg} \theta + (I_2 - j_2)j_3] \sum_{h=0}^{\infty} g_k'(R^2, j^2) j_s^{2h} \\
&\quad - 2j_2 j_3 \sum_{h=1}^{\infty} k g_k(R^2, j^2) j_s^{2(h-1)}, \\
\dot{j}_2 &= 2(I_1 - j_1)(j_1 \operatorname{ctg} \theta + j_3) \sum_{h=0}^{\infty} g_k'(R^2, j^2) j_s^{2h} + 2j_1 j_3 \\
&\quad \times \sum_{h=1}^{\infty} k g_k(R^2, j^2) j_s^{2(h-1)}, \\
\dot{\theta} &= 2(I_2 - j_2) \sum_{h=0}^{\infty} g_k'(R^2, j^2) j_s^{2h}, \\
\dot{\phi} &= -2 \frac{I_1 - j_1}{\sin \theta} \sum_{h=0}^{\infty} g_k'(R^2, j^2) j_s^{2h}. \quad (16)
\end{aligned}$$

These equations have three constants of motion, namely, I^2 , j^2 , and $I_3 = j_3$, where the last of these is connected with the absence of rotation around the symmetry axis. Moreover, they are invariant under rotations by 180° around ICF axis 1 and 2. The stationary states of (16) are identical with the stationary states of the energy surface (7).

PRECESSION NEAR AN ALIGNED CONFIGURATION

The linearized set of equations for the small first-order quantities $I_2, j_2, j_3, = I_3$, and $\delta\theta = \pi/2 - \theta$ takes the form

$$\begin{aligned}
\dot{I}_2 &= \Omega(j_3 + I\delta\theta), \\
\dot{j}_2 &= \Omega(j_3 + j\delta\theta) + 2j_1 j_3 g_1(R_-^2, j^2), \\
\dot{j}_3 &= 2(j_1 I_2 - I_1 j_2) g_0'(R_-^2, j^2), \quad (17)
\end{aligned}$$

$$\delta\dot{\theta} = -2(I_2 - j_2)g_0'(R^{-2}, j^2),$$

where

$$\Omega = \partial E_0 / \partial I = 2(I - j)g_0'(R^{-2}, j^2) \quad (18)$$

is the rotational frequency of the core. Equations (17) describe two normal oscillations. The oscillation of frequency Ω is the zeroth mode: the vectors \mathbf{I} and \mathbf{j} are oriented along a straight line that oscillates in the plane perpendicular to the symmetry axis.

After the zeroth mode, we have the normal oscillation with frequency

$$\omega_{>} = [\Omega^2 + 4Ijg_1(R^{-2}, j^2)g_0'(R^{-2}, j^2)]^{1/2}, \quad (19)$$

for which the solution of (17) is

$$I_2(t) = 0, \quad j_2(t) = -\frac{\alpha j \omega_{>}}{2I g_0'(R^{-2}, j^2)} \cos \omega_{>} t, \quad (20)$$

$$I_3(t) = j_3(t) = \alpha j \sin \omega_{>} t, \quad \delta\theta(t) = -I_3(t)/I,$$

where α is an arbitrary small quantity that determines the precession amplitude, and the increments on I_1 and j_1 are proportional to α^2 . These oscillations are shown in Fig. 1: the vectors \mathbf{I} and \mathbf{R} oscillate relative to axis 1 in the 1, 3 and 1, 2 planes, respectively, and \mathbf{j} describes an elliptical cone around axis 1. Consequently, the motion of all these vectors is localized near ICF axis 1.

The last equation in (16) enables us to determine the time dependence of the azimuthal angle ϕ and, consequently, the motion of the symmetry axis as well:

$$n_x = \sin \theta \cos \varphi \approx \cos \Omega t, \quad n_y = \sin \theta \sin \varphi \approx -\sin \Omega t, \quad (21)$$

$$n_z = \cos \theta \approx -\alpha(j/I) \sin \omega_{>} t.$$

This means that the vector \mathbf{n} rotates clockwise (the moment of inertia \mathbf{I} points in the negative direction of the z axis) with frequency in the x, y plane, whereas the oscillations of frequency $\omega_{>}$ take it out of this plane.

The probability of $M1$ transitions between levels in neighboring multiplets is determined by the components of the operator \mathbf{j} along the LCS axes. Here, it is interesting to examine the time dependence of the classical angular momentum \mathbf{j} . It can be found by transforming the vector \mathbf{j} from the ICF to LCS. For the component $j_{+1} = j_x + ij_y$, in which we are interested here, we have

$$j_{+1}(t) = -i\alpha j \{ (\Omega + \omega_{>}) \exp[-i(\Omega - \omega_{>})t] - (\Omega - \omega_{>}) \times \exp[-i(\Omega + \omega_{>})t] \} / 4I g_0'(R^{-2}, j^2). \quad (22)$$

It is important to note that the precessional motion relative to the aligned configuration (10) does not depend on the $k > 2$ terms in the Hamiltonian (1), which are responsible for the change in the mean field of the core as a result of rotation. This enables us to compare our present results with the harmonic approximation, obtained using the algebra of the angular momentum operators \mathbf{I} and \mathbf{j} in Refs. 14 and 15 [which is different from (2)] for the simple Hamiltonian of the particle-plus-core model

$$H = A\mathbf{R}^2 + Cj_3^2, \quad (23)$$

where A and C are constants.

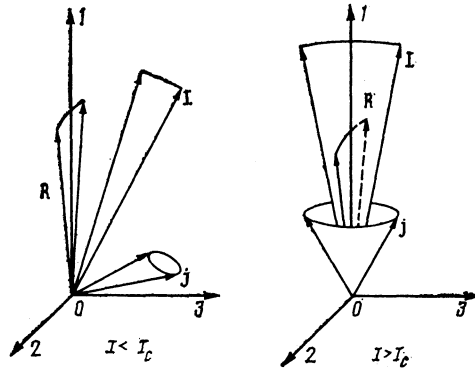


FIG. 1. Two regimes of precessional motion of vectors \mathbf{I} , \mathbf{R} , and \mathbf{j} , relative to the ICF on either side of the critical point I_c .

PRECESSION NEAR ONE OF THE DEGENERATE STATES

As I approaches the critical value I_c , the frequency $\omega_{>}$ decreases in proportion to $(I - I_c)^{1/2}$, and the oscillation amplitudes of vectors \mathbf{I} and \mathbf{j} in the direction of axis 3 increase without limit. For $I < I_c$, the aligned configuration (10) becomes unstable, and the vectors \mathbf{I} and \mathbf{j} begin to precess around one of the stationary states (14). After the zeroth mode has been extracted, the linearized equations for a normal oscillation of frequency

$$\omega_{<} = \left\{ \frac{4A}{I_{10}j_{10}} j_{30}^2 [-CR_0^2 + 2A'R_0^4 + 4C'R_0^2 I_{10}j_{10} + 2DI_{10}^2 j_{10}^2] \right\}^{1/2} \quad (24)$$

have the form

$$\dot{j}_2 = \frac{\omega_{<}^2}{2AI_{10}} \delta j_3, \quad \dot{\delta j}_3 = -2AI_{10} j_2, \quad (25)$$

where $\delta j_3 = j_3 - j_{30}$. The coefficients A and C in this expression are determined by (9) for the equilibrium value ϑ_0 of ϑ and

$$A' = \sum_{h=0}^{\infty} j_{30}^{2h} g_h''(R_0^2, j^2), \quad C' = \sum_{h=0}^{\infty} k j_{30}^{2h-2} g_h'(R_0^2, j^2), \quad (26)$$

$$D = \sum_{h=0}^{\infty} k(k-1) j_{30}^{2h-4} g_h(R_0^2, j^2).$$

Near the critical point j_{30}^2 is small, so that we can find an analytic solution of (8) for the stationary state (14). In this limit, the precession frequency $\omega_{<}$, which is proportional to $(I_c - I)^{1/2}$, depends only on the five constants $g_0'(I_c)$, $g_0''(I_c)$, $g_1(I_c)$, $g_1'(I_c)$, and $g_2(I_c)$.

The time dependence of the components of the vectors \mathbf{I} and \mathbf{j} along the ICF axis is described by the formula

$$I_1(t) = I_{10} - \alpha j \frac{j_{30}}{I_{10}} \sin \omega_{<} t, \quad j_1(t) = j_{10} - \alpha j \frac{j_{30}}{j_{10}} \sin \omega_{<} t, \quad (27)$$

$$I_2(t) = 0, \quad j_2(t) = -\alpha \frac{j \omega_{<}}{2AI_{10}} \cos \omega_{<} t,$$

$$I_3(t) = j_3(t) = j_{30} + \alpha j \sin \omega_{<} t,$$

and

$$\theta(t) = \theta_0 - \alpha \frac{j}{I_{10}} \sin \omega_{\leftarrow} t, \quad \text{ctg } \theta_0 = -\frac{j_{30}}{I_{10}}. \quad (28)$$

Consequently, the vector \mathbf{I} oscillates in the 1, 3, plane around the stationary position \mathbf{I}_0 , and the vector \mathbf{R} oscillates in the 1, 2, plane around axis 1; the vector \mathbf{j} describes an elliptical cone around \mathbf{j}_0 . In contrast to the precession in the region $I > I_c$, the motion of all three vectors is now localized in different regions of space (see Fig. 1 which shows the precession near the stationary state with $j_{30} > 0$). The time dependence of the component j_{+1} of vector \mathbf{j} in LCF has the form

$$j_{+1}(t) = \frac{j_{30}}{I} (I_{10} - j_{10}) e^{-i\Omega_1 t} + i\alpha j \{ S e^{-i(\Omega_1 - \omega_{\leftarrow})t} + Q e^{-i(\Omega_1 + \omega_{\leftarrow})t} \}, \quad (29)$$

where $\Omega_1 = \partial \tilde{E}_0 / \partial I = 2AI(I_{10} - j_{10})/I_{10}$ is the rotational frequency of the core and the quantities S and Q depend on the values of the components of \mathbf{I}_0 and \mathbf{j}_0 along the ICF axis.

4. QUANTUM-MECHANICAL BIFURCATION

For the quantum-mechanical description of the above bifurcation, let us simplify the effective Hamiltonian (1) by recalling that the bifurcation occurs in a small part of phase space corresponding to low-lying RM states $|In\rangle$ for which

$$\langle In | \mathbf{R}^2 - R_-^2 | In \rangle / I(I+1) \ll 1.$$

Near the critical point, these states are described by the Hamiltonian

$$H = E_0(I) + a_1(\mathbf{R}^2 - R_-^2) + a_2(\mathbf{R}^2 - R_-^2)^2 + b_1 j_3^2 + \frac{1}{2} b_2 [\mathbf{R}^2 - R_-^2; j_3^2] + c_1 j_3^4, \quad (30)$$

which is obtained from (1) by expanding the functions g_k^+ ($k = 0, 1, 2$) near the aligned state into a series in powers of $\mathbf{R}^2 - R_-^2$. The terms that we have written out are sufficient to describe the bifurcation, and this can be demonstrated by estimating the higher-order expansion terms as was done in Ref. 16.

The regular part E_0 of (30) is the energy of the lowest RM state of the aligned band in the limit $I \gg 1$ [see (11)]. The remaining five constants are determined by the structure of the nucleus as a whole, and can be obtained in the course of the reduction of its total Hamiltonian. They have a perfectly definite physical meaning. The constants a_1 and a_2 are the rotational parameters in the expansion of the energy of an even-even nucleus in terms of the square of the angular momentum. The constants b_1 and c_1 determine the level splitting in the j -subshell by the quadrupole and hexadecapole deformation of the nucleus. Finally, the term proportional to the constant b_2 describes the variation of the Coriolis interaction across the band. In the region of the rotational anomaly (backbending), in which the interaction between single-quasiparticle and three-quasiparticle excitations is significant, the Hamiltonian (30) and the original Hamiltonian (1) are no longer satisfactory.

To elucidate the nature of the change in the dynamics of the band under investigation, we must first establish the solutions of the Hamiltonian (30) in the harmonic approximation. We do this by the method developed in Ref. 17. We seek

the solution of the Schrodinger equation with the Hamiltonian (30) in the form given by (4). Since the quantity

$$\delta = [I(I+1)]^{-1/2}, \quad (31)$$

is small, we pass from the recurrence relation for coefficients a_{IKn} to the differential equations for the function

$$a_{In}(k) = s^{-1/2}(k) \psi_n(x), \quad (32)$$

where

$$k = \delta K, \quad x = \delta^{-1} \int s^{-1/2}(k) dk, \\ s(k) = \left[1 + 4\delta^{-2} \frac{a_2}{a_1} (\mu - k^2) + \delta^{-2} \frac{b_2}{a_1} k^2 \right] [(1 - k^2)(\mu^2 - k^2)]^{1/2} - 4\delta^{-2} \frac{a_2}{a_1} (1 - k^2)(\mu^2 - k^2), \\ \mu = \delta [j(j+1)]^{1/2}. \quad (33)$$

After some relative simple manipulations, we obtain the following equation for the Ψ function:

$$\frac{d^2 \psi_n}{dx^2} + [e - V(x)] \psi_n(x) = 0, \quad e = \frac{E - E_0}{I(I+1)a_1}. \quad (34)$$

This equation was obtained from the five-term recurrence relation and is valid only in the harmonic approximation when the potential

$$V = 2(\mu - k^2) + \frac{b_1}{a_1} k^2 + 4\delta^{-2} \frac{a_2}{a_1} [2\mu^2 - (1 + \mu)^2 k^2 + 2k^4] + 2\delta^{-2} \frac{b_2}{a_1} k^2 (\mu - k^2) + \delta^{-2} \frac{c_1}{a_1} k^4 - 2 \left[1 + 4\delta^{-2} \frac{a_2}{a_1} (\mu - k^2) + \delta^{-2} \frac{b_2}{a_1} k^2 \right] [(1 - k^2)(\mu^2 - k^2)]^{1/2} \quad (35)$$

is a quadratic in x . The stationary states (10) and (14) correspond to the minimum of the potential (35). This means that, by expanding it around the stationary points, we can investigate the quantum-mechanical precession of the angular momenta. This is described by the wave function (4) with the coefficients given by (32) in which $\psi_n(x)$ are the wave functions of the simple harmonic oscillator.¹⁸

Let us now examine the structural change in the quantum-mechanical RM states as I increases within the band in which bifurcation occurs at the critical point I_c . The low-lying levels in the band with $I < j$ are described by the strong coupling scheme and are of no interest for the phenomenon investigated here.

QUANTUM-MECHANICAL PRECESSION FOR $j < I < I_c$

In this range, the angular momentum \mathbf{j} breaks away from the symmetry axis (when \mathbf{j} is high enough) and the stationary state (14) is established. The two degenerate minima of the potential (35) at the point $\pm k_0$ correspond to this state. The energy of the low-lying RM levels is given by

$$E_n(I) = E_0(I) + a_1 I(I+1) V(k_0) + \omega_{\leftarrow}(I) (n + 1/2), \quad (36)$$

where the precession frequency is

$$\omega_{<} = (I + 1/2) a_1 [2\delta(k_0) V''(k_0)]^{1/2} \quad (37)$$

and becomes identical with (24) in the classical limit if we take into account the difference between the Hamiltonians (1) and (30). The above formulas refer to motion in one of the wells, and determine the corresponding values of the Hamiltonian (30) with broken C_2 symmetry. To improve the approximation, we can use instead of (32) the symmetrized combinations

$$a_{I_n}(k) = s^{-1/2}(k) \{ \psi_n(x-x_0) + (-1)^{I-j-n} \psi_n(x+x_0) \} / 2^{1/2} \\ \times [1 + (-1)^{I-j-n} J_n]^{1/2}, \quad (38)$$

where x_0 is the equilibrium position corresponding to k_0 and J_n is the overlap integral of the functions $\psi_n(x-x_0)$ and $\psi_n(x+x_0)$. Averaging the Hamiltonian (30) over the projection functions (38), we can find the exponentially small increments on the energies of the lowest-lying RM levels that depend on the signature. They appear because the angular momenta I and j can tunnel through the barrier between the two degenerate stationary states. Consequently, in the region that we are considering, the $E_n^{(+)}(I)$ and $E_n^{(-)}(I)$ curves that correspond to the energies of the low-lying RM levels with different signatures approach one another.

We shall now use the expressions given by (32) for the coefficients a_{IK_n} to evaluate the probabilities of electromagnetic transitions in a band. The technique for doing this reduces to the replacement of the summation over K with integration with respect to x , and the expansion of the integrand into a series in the small deviation x . The final expression for the reduced transition probability takes the form of a series in powers of the small parameter δ given by (31).

For $I < I_c$, there are according to (29) three types of $M1$ transition with frequencies Ω and $\Omega \pm \omega_{<}$, respectively. The transition frequency between levels in neighboring RM with equal quantum numbers n is Ω (if we ignore exponentially small terms). The reduced probability of such transitions is

$$B(M1, I_n \rightarrow I-1 n) = \frac{3}{8\pi} \mu_N^2 (g_j - g_R)^2 \\ \times I(I+1) k_0^2 [(1 - k_0^2)^{1/2} - (\mu^2 - k_0^2)^{1/2}]^2, \quad (39)$$

where μ_N is the nuclear magnetism, g_R is the collective gyromagnetic ratio, and $g_j = g_l + (g_s - g_l)/(2j + 1 \mp 1)$ for $j = l \pm 1/2$ (g_l and g_s are the orbital and spin gyromagnetic ratios of the nucleon). In accordance with the classical expression (29), this reduced probability has a smooth dependence on I . Transitions of this type between the lowest-lying levels of neighboring RM are observed experimentally. $M1$ transitions between levels with quantum numbers I_n and $I-1 n \pm 1$ and with combination frequencies $\Omega \pm \omega_{<}$ should depend on the signature as indicated by (29). These transitions involve not only the lowest-lying RM levels, but also other levels, so that they are not observed experimentally. A similar method can be used to evaluate the $E2$ transitions, and the electric quadrupole and magnetic dipole moments in a band. $E2$ transitions between levels with the same n and also the static moments should have a smooth dependence on I .

QUANTUM-MECHANICAL PRECESSION FOR $I > I_c$

The stationary state (10) corresponds to the minimum of the potential for $k = x = 0$. Simple manipulation then leads to the following relation for the energy of the lowest-lying levels in the multiplet:

$$E_n(I) = E_0(I) + \omega_{>}(I) (n + 1/2), \quad (40)$$

where the frequency is

$$\omega_{>}(I) = 2 [a_1^2 (I-j)^2 + a_1 b_1 (I + 1/2) (j + 1/2)]^{1/2} \quad (41)$$

and becomes identical with the classical formula (19) when I and j are large. Since the coefficients a_K have the symmetry properties indicated by (5), we find that the parity of the quantum number n is the same as the parity of $I - j$. Hence the lowest-lying RM levels with even $I - j$ have $n = 0, 2, 4, \dots$ (favored band) and those with odd values of this difference have $n = 1, 3, 5, \dots$ (unfavored band).

There are two types of $M1$ transition in a band. Their frequencies are $\Omega + \omega_{>}$ and $\Omega - \omega_{>}$ and the corresponding reduced probabilities are

$$B(M1; I_n \rightarrow I-1 n \pm 1) = \frac{3}{8\pi} \mu_N^2 (g_j - g_R)^2 \frac{(2j+1) a_1}{(2I+1) \omega_{>}} \\ \times \left(I - j \pm \frac{\omega_{>}}{2a_1} \right)^2 \left(n + \frac{1}{2} \pm \frac{1}{2} \right). \quad (42)$$

For $I \gg j$ it then follows from (41) that $\omega_{>}(I) \approx 2a_1(I-j) = \Omega$. Hence, the $M1$ transitions with frequencies $\Omega + \omega_{>}$ (unfavored-favored), which by (41) are proportional to $(1 - \omega_{>}/\Omega)^2$, are highly suppressed as compared with the transitions of frequency $\Omega - \omega_{>}$ (favored-unfavored). Consequently, we should observe a characteristic zigzag dependence on I for the reduced transition probabilities (42). The reason for this behavior can be elucidated by considering the expression for the classical quantity $j_{+1}(t)$ given by (22), whose Fourier components determine the transition probability.¹⁹ The $E2$ transition probability between low-lying levels of neighboring multiplets and the static moments in a band do not have as well-defined zigzag dependence as the $M1$ transitions because the oscillating terms in the expressions for these quantities are proportional to the small parameter δ . We emphasize that the energies, static moments, and transition probabilities in an aligned band do not depend in the harmonic approximation on effects associated with the nonadiabatic rotation of the core, the change in the Coriolis interaction (the constant b_2), or the hexadecapole deformation.

The harmonic approximation thus enables us to follow the qualitative changes in the spectrum of rotational excitations that accompany the quantum-mechanical bifurcation. The mutual approach of the $E_n^{(+)}(I)$ and $E_n^{(-)}(I)$, curves that correspond to levels with different signature (favored, unfavored), and the change in the nature of the dependence on I in $M1$ transition probabilities between these levels, which is responsible for the zigzag on the smooth variation as the critical point is crossed from right to left, can be regarded as the bifurcation criteria.

The harmonic approximation is invalid in the neighborhood of the critical point, and the exact solutions corresponding to the Hamiltonian (30) must be used to follow how these qualitative changes take place. Figure 2 shows the

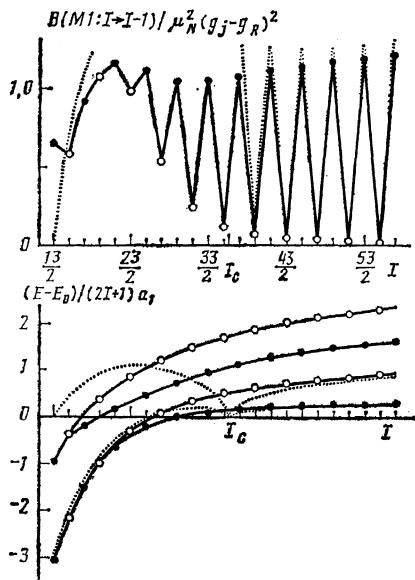


FIG. 2. Energies of low-lying levels in rotational multiplets and the reduced $M1$ transition probabilities between low-lying levels near the critical point I_c , calculated for the following values of the parameters of the effective Hamiltonian (30): $b_1/a_1 = -1.0$, $a_2/a_1 = -2 \times 10^{-4}$, $b_2/a_1 = -10^{-4}$, $c_1/a_1 = -5 \cdot 10^{-3}$. The solid line joins the following points: ●—even $I-j$, ○—odd $I-j$. The dotted line represents the harmonic approximation.

energies and reduced $M1$ transition probabilities as a functions of I near the critical point I_c . These curves were obtained by numerical diagonalization of the Hamiltonian and by using the harmonic approximation. The mutual approach of levels of opposite parity is not very clear in comparison with the fast variation in the level energy in multiplets with different I . To exhibit this effect we must remove the regular part containing the main dependence on I from the energy $E_n(I)$. It is convenient to take this to be the energy $E_0(I)$ of the lowest level in the aligned configuration. The difference $E - E_0$ for the precessional motion in the region $I > I_c$ is then shown by (40) and (41) to increase in proportion to the first power of the angular momentum, whereas the dimensionless quantity $[E(I) - E_0(I)]/a_1(2I + 1)$ remains constant in the limit of large I . On the contrary, for $I < I_c$, this quantity is proportional to I since $V(k_0)$ in (36) is negative and its absolute magnitude decreases as I approaches I_c . It is thus clear why a set of equidistant levels, shifted relative to the origin by half the separation between them, i.e., $(\omega_>(I)/2a_1(2I + 1))$, appears on the right hand side of the lower graph of Fig. 2. The difference between Fig. 2 and the harmonic approximation is that there is now a transition region between different regimes of precessional motion. The width of this region decreases as the size of the configuration space of states on the right hand side of (4), i.e., the quantum number j , increases.

In numerical calculations, the constants in the Hamiltonian (30) were assumed to have values typical for all the deformed nuclei of the isotopes of Dy, Er, and Yb with deformation parameters $\beta_2 \approx 0.3$, $|\beta_4| \approx 0.05$. The values $a_1 \sim 10$ keV, $a_2 \sim a_1 \cdot 10^{-4}$ keV are typical for the even-even isotopes of these nuclei. We note that a_1 and a_2 can also be determined as the coefficients of the expansion for the rotational level energy of an aligned band in an odd nucleus:

$$E = E_1 + a_1(I-j)^2 + a_2(I-j)^4 + \dots \quad (43)$$

The parameter b_1 determines the level splitting of a subshell in the quadrupole field of the nucleus:

$$b_1 = \frac{3\kappa_2 \beta_2}{j(j+1)} (u_j^2 - v_j^2), \quad (44)$$

where $\kappa_2 \approx 8$ MeV and the factor that depends on the amplitudes u and v of the Bogolyubov transformation determines the occupancy of the j -level. The constant

$$c_1 = 9\kappa_4 \beta_4 (u_j^2 - v_j^2) / (j-1)j(j+1)(j+2) \quad (45)$$

in the Hamiltonian is responsible for the level splitting in the hexadecapole field. To estimate κ_4 , we can use the relation $\kappa_4 = -2\kappa_2$ which is valid for a potential well with infinitely high walls. Formulas (44) and (45) lead to the following estimates for $j = 13/2$:

$$b_1/a_1 \sim 10(u_j^2 - v_j^2), \quad |c_1|/b_1 \leq 2 \cdot 10^{-2}. \quad (46)$$

For an isolated j -level, bifurcation occurs only when $b_1 < 0$, i.e., the subshell is more than half filled. The greater the absolute value of $p = b_1/2a_1$, the greater the critical moment of inertia I_c (13) and the more developed the region in which the doubly degenerate stationary states (14) can exist. Variations in the constants b_2 and c_1 appear mostly for $I < I_c$. The separation between these two curves is also a function of the parameter b_2 . The effect of increasing non-adiabaticity of rotation (the constant a_2) is greater for the higher members of a multiplet and eventually leads to an increase in the anharmonicity of the precession spectra.

The reduced separation between these curves, which is observed for low-lying levels in multiplets, and is typical for bifurcation, can be seen in bands based on one-quasiparticle states in the upper part of the subshell with anomalous parity. Figure 3 shows experimental data, taken from Refs. 20–

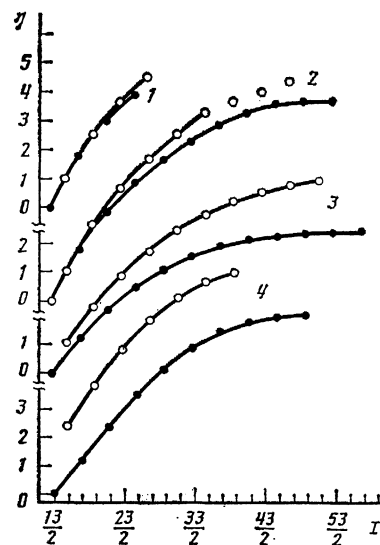


FIG. 3. Onset of bifurcation in the rotational spectra of the odd isotopes of Yb as the number of neutrons in the nucleus increases. The solid line joins the experimental points with even (●) and odd (○) values of the difference $I-j$: 1 is the $7/2^+$ (633) band of the nucleus $^{171}\text{Yb}_{101}$; 2 is the same band for $^{169}\text{Yb}_{99}$, 3 is the $5/2^+$ [642] band of $^{167}\text{Yb}_{97}$, and 4 is the $3/2^+$ [651] band of $^{163}\text{Yb}_{93}$.

22, on the rotational bands of the isotopes of Yb with an odd number of neutrons. We have selected bands based on states with quantum numbers $K^\pi [Nn_z \Lambda]$ in the $i_{13/2}$ subshell. In each band, we analyzed levels with spin between $I = 13/2$ and the maximum values of I which, however, lay below the region of the first rotational anomaly (backbending). This limitation ensured that the phenomenological theory based on the Hamiltonian (30) remained valid. The mutual approach of the $E_0^{(+)}(I)$ and $E_0^{(-)}(I)$ curves can be seen by investigating the I dependence of the quantity

$$\eta = \{E(I) - E(j) - a_1(I-j)^2\} / a_1(2I+1), \quad (47)$$

where $E(I)$ is the level energy in a band. In contrast to Fig. 2, the energy in (47) is measured from the level with $I = j = 13/2$ because the graphical representation is then more convenient. The rotational constant a_1 in (47) was determined from the rotational levels of the aligned part of the band. The coalescence of curves corresponding to level sequences with odd and even values of the difference $I-j$ serves as an indicator of the mutual approach of the $E_0^{(+)}(I)$ and $E_0^{(-)}(I)$ curves.

As the number of neutrons in the Yb isotopes increases, the levels in the $i_{13/2}$ subshells with increasing quantum number K become filled, the Fermi surface rises above the midpoint of the subshell, and the constant b_1 in (44) becomes negative. The critical moment of inertia I_c increases as the absolute magnitude of b_1 increases and the effect of the mutual approach of the $E_0^{(+)}(I)$ and $E_0^{(-)}(I)$ curves becomes more noticeable.

It is clear from Fig. 3 that bifurcation occurs for neutron numbers in the range 97–99, for which the occupancy of the subshell is close to one-half. In the aligned part of the ^{169}Yb band, the level sequence with odd $I-j$ shows an irregularity in the disposition of levels (the corresponding points are not joined together in the figure). The reason for this anomaly, which is unrelated to bifurcation, is still not clear.

The mutual approach of the curves is more clearly defined in ^{171}Yb than in ^{169}Yb , although the occupancy of the $i_{13/2}$ subshell is the same in the two nuclei. This can be ex-

plained by a reduction in b_1 in (44) due to the fact that the Fermi surface has risen as a result of the addition of two neutrons. A further possible factor that brings these curves closer together is the negative hexadecapole deformation ($\beta_4 = 0$ and $\beta_4 = -0.02$ for ^{168}Yb and ^{170}Yb , respectively). According to (45), this should increase the j -level splitting. The constants in the Hamiltonian (30) are thus seen to be determined by internal nuclear dynamics, and the bifurcation phenomenon that we have considered is a many-particle effect.

- ¹R. Gilmore and D. H. Feng, Nucl. Phys. A **301**, 189 (1979).
- ²D. H. Feng, R. Gilmore, and S. R. Deans, Phys. Rev. C **23**, 1254 (1981).
- ³Zhang Wei-Man, D. H. Feng, and J. N. Ginocchio, Phys. Rev. C **37**, 1281 (1988).
- ⁴S. T. Belyaev and I. M. Pavlichenkov, Nucl. Phys. A **388**, 505 (1982).
- ⁵R. Gilmore, S. Kais, and R. D. Levine, Phys. Rev. A **34**, 2442 (1986).
- ⁶V. I. Zhilinskii and I. M. Pavlichenkov, Zh. Eksp. Teor. Fiz. **92**, 287 (1987) [Sov. Phys. —JETP **65**, 221 (1987)].
- ⁷I. M. Pavlichenkov and B. I. Zhilinskii, Chem. Phys. **100**, 339 (1985).
- ⁸D. A. Sadovskii and B. I. Zhilinskii, Molec. Phys. **65**, 109 (1988).
- ⁹V. I. Zhilinskii and I. M. Pavlichenkov, Opt. Spektrosk. **64**, 688 (1988) [Opt. Spectrosc. (USSR) **64**, 413 (1988)].
- ¹⁰I. Hamamoto and B. Mottelson, Phys. Lett. B **127**, 281 (1983); **132**, 7 (1986); **167**, 370 (1986).
- ¹¹I. Hamamoto, Phys. Lett. B **179**, 327 (1986).
- ¹²W. Kotos and L. Wolniewicz, Rev. Mod. Phys. **35**, 473 (1963).
- ¹³A. Bohr and B. R. Mottelson, Nuclear Structure, Benjamin, Reading, 1975 [Russ. transl. Mir, Moscow, 1988].
- ¹⁴A. Bohr and B. R. Mottelson, Phys. Scripta **22**, 461 (1980).
- ¹⁵E. R. Marshalek, Phys. Rev. C **26**, 1678 (1982).
- ¹⁶I. M. Pavlichenkov and B. I. Zhilinskii, Ann. Phys. (N. Y.) **184**, 1 (1988).
- ¹⁷P. A. Braun, A. M. Shirokov, and Yu. F. Smirnov, Molec. Phys. **56**, 537 (1985).
- ¹⁸L. D. Landau and E. M. Lifshitz, Quantum Mechanics, Pergamon Press, Oxford, 1972 [Russ. original, Nauka, Moscow, 1974].
- ¹⁹I. Hamamoto, Phys. Lett. B **102**, 255 (1981).
- ²⁰Th. Liudblad, H. Ryde, and D. Barneoud, Nucl. Phys. A **193**, 155 (1972).
- ²¹J. Kownacki, J. D. Garrett, J. J. Gaardhoje *et al.*, Nucl. Phys. A **394**, 269 (1983).
- ²²J. C. Bacelar, M. Diebel, C. Ellegaard *et al.*, Nucl. Phys. A **442**, 509 (1985).

Translated by S. Chomet